

D. G. Kamper, E. G. Cruz and M. P. Siegel

J Neurophysiol 90:3702-3710, 2003. First published Sep 3, 2003; doi:10.1152/jn.00546.2003

You might find this additional information useful...

This article cites 38 articles, 10 of which you can access free at:

<http://jn.physiology.org/cgi/content/full/90/6/3702#BIBL>

This article has been cited by 2 other HighWire hosted articles:

Kinematic and Dynamic Synergies of Human Precision-Grip Movements

I. V. Grinyagin, E. V. Biryukova and M. A. Maier
J Neurophysiol, October 1, 2005; 94 (4): 2284-2294.
[\[Abstract\]](#) [\[Full Text\]](#) [\[PDF\]](#)

Kinetic and kinematic workspaces of the index finger following stroke

E. G. Cruz, H. C. Waldinger and D. G. Kamper
Brain, May 1, 2005; 128 (5): 1112-1121.
[\[Abstract\]](#) [\[Full Text\]](#) [\[PDF\]](#)

Updated information and services including high-resolution figures, can be found at:

<http://jn.physiology.org/cgi/content/full/90/6/3702>

Additional material and information about *Journal of Neurophysiology* can be found at:

<http://www.the-aps.org/publications/jn>

This information is current as of May 14, 2010 .

Stereotypical Fingertip Trajectories During Grasp

D. G. Kamper,^{1,2} E. G. Cruz,² and M. P. Siegel²

¹Department of Physical Medicine and Rehabilitation, Feinberg School of Medicine, Northwestern University, Chicago; and ²Sensory Motor Performance Program, Rehabilitation Institute of Chicago, Chicago, Illinois 60611

Submitted 4 June 2003; accepted in final form 29 August 2003

Kamper, D. G., E. G. Cruz, and M. P. Siegel. Stereotypical fingertip trajectories during grasp. *J Neurophysiol* 90: 3702–3710, 2003. First published September 3, 2003; 10.1152/jn.00546.2003. The kinematics of movement of all five digits was analyzed during reach-and-grasp tasks for a variety of objects. Ten healthy subjects performed 20 trials involving the grasp of five objects of distinct size and shape. Joint angles were recorded, and digit trajectories were computed using forward kinematics. For a given subject, fingertip trajectories were consistent across trials. The different-sized objects largely produced movement along different portions of a stereotypical trajectory described by a logarithmic spiral. The spirals fit the actual finger positions with a mean error across all trials of 0.23 ± 0.25 cm and accounted for over 98% of the variance in finger position. These patterns were consistent independent of initial finger posture. Subjects did not produce straight-line movements, either in Cartesian space or joint space. The direction of the thumb trajectories exhibited a greater dependence on object type than the finger trajectories, but still utilized a small percentage (<5%) of the available workspace. These results suggest that restoration of a small but specific part of the workspace could have significant impact on function following hand impairment.

INTRODUCTION

The human hand is comprised of many joints that permit an infinite number of different trajectories to move the fingers from one location in space to another. It is this ability that makes the hand so valuable in many daily tasks.

However, this freedom adds a layer of complexity to the control scheme, as a particular trajectory must be selectively planned and executed. Some researchers suggest that the nervous system typically reduces the potential solution space for multi-joint movements by using specific patterns of activation, or synergies (Latash et al. 2002b; Li et al. 1998).

Certainly, patterns of movement often emerge in a variety of upper extremity tasks. During planar reaching, for example, subjects have exhibited a tendency to produce a straight-line hand movement between two points (Flash and Hogan 1985; Wolpert et al. 1995), with a single peak in the tangential velocity curve (Morasso 1981). A number of planning strategies have been proposed to account for these consistent patterns. These include efforts to minimize jerk in the movement (Flash and Hogan 1985), change in joint torque (Uno et al. 1989), or discomfort (Cruse et al. 1990; for a review, see Engelbrecht 2001).

Researchers have observed characteristic hand postures dur-

ing grasping as well. In reach-to-grasp tasks, the aperture between the thumb and index finger has often been used to describe the grasp. When the task is initiated with the index finger and thumb in contact, the aperture between them typically shows a trajectory with a single peak with characteristic timing (Gentilucci et al. 1992; Haggard and Wing 1995; Jeannerod 1984).

A limited set of joint configurations has been shown to provide a basis for a variety of grasping tasks (Santello et al. 1998, 2002) and typing (Soechting and Flanders 1997). Similarly, a few eigenpostures with temporal weightings were sufficient to describe hand configurations during reach-to-grasp movements for a variety of objects (Mason et al. 2001).

However, the fingertip trajectories with respect to the hand during the reach-to-grasp tasks have not been well described. We were interested in whether stereotypical movement patterns might be present, and if so, whether these patterns would be similar to those observed for hand movement with respect to the shoulder.

This study attempted to characterize motion of the digits during grasping. Subjects performed multiple trials for objects of varying size and shape in as natural a manner as possible, with no constraints on forearm or wrist orientation or on grasping strategy. Fingertip motion followed a stereotypical trajectory, which could be described with a basic mathematical function. The trajectory was largely unaffected by initial finger posture.

METHODS

Ten subjects (age, 21–32 yr) with no sign of neurological or joint impairment participated in a series of grasping tasks. The gender distribution of the subjects was eight males and two females. Five different objects were employed: a plastic cup (diameter varying from 9 to 6.6 cm), a softball (9.7 cm diam), a marker (1.7 cm diam), a standard playing card, and a CD (12 cm diam) (Santello et al. 1998). The objects were arranged on a table at which the subject sat. The cup was upright, the marker was flat on the table, and the CD was positioned atop a 2-cm pedestal that kept the CD parallel with the tabletop. The playing card, situated atop a deck of cards, had roughly 3 cm overhanging the deck, so that the card was accessible from underneath, above, and the sides.

Every subject performed 20 grasping trials. The participant was instructed to either grasp a single object (10 trials) or all five objects in succession (10 trials). Object order between and within trials was randomly selected. Subjects rested for 1 min between each trial.

Address for reprint requests and other correspondence: D. Kamper, Sensory Motor Performance Program, Rehabilitation Institute of Chicago, Suite 1406, 345 E. Superior St., Chicago, IL 60611 (E-mail: d-kamper@northwestern.edu).

The costs of publication of this article were defrayed in part by the payment of page charges. The article must therefore be hereby marked “advertisement” in accordance with 18 U.S.C. Section 1734 solely to indicate this fact.

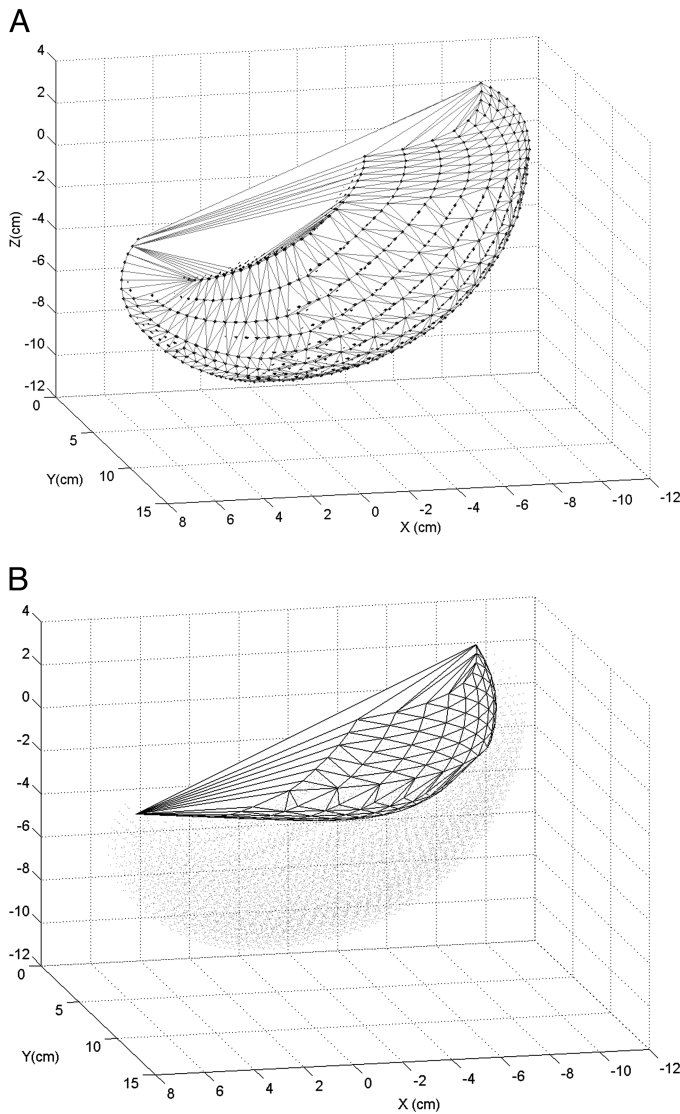


FIG. 1. Estimation of volume of potential thumb workspace. Workspace was spanned through forward kinematics. Convex hulls (mesh) were fit to (A) convex and (B) concave surfaces of the space. Lighter dots in B represent thumb workspace. Workspace volume was found by subtracting volume encompassed by the hull in B from volume encompassed by the hull in A.

For each trial, the participant was told to begin with his/her hand placed in a relaxed posture on the thigh. Once instructed to move, the subject reached for the appropriate object, which he or she lightly grasped as though to lift. No instructions regarding use of specific fingers or specific arm orientations were given. Thus the subjects were free to approach and contact the object in any manner they deemed appropriate. Participants were told not to actually lift or squeeze the object on grasping, in an effort to focus on planned fingertip trajectories, distinct from the finger motion that might result from forceful

TABLE 1. Starting finger posture across all subjects

Finger	MCP	Joint PIP	DIP
Index	5.2 ± 6.5°	10.5 ± 4.8°	1.1 ± 2.5°
Middle	-1.4 ± 6.5°	8.4 ± 5.4°	1.9 ± 2.2°
Ring	0.6 ± 6.0°	6.5 ± 3.2°	1.6 ± 2.6°
Little	3.8 ± 6.7°	3.1 ± 4.5°	1.4 ± 1.9°

Values are mean ± SD. Joint flexion is positive and extension is negative.

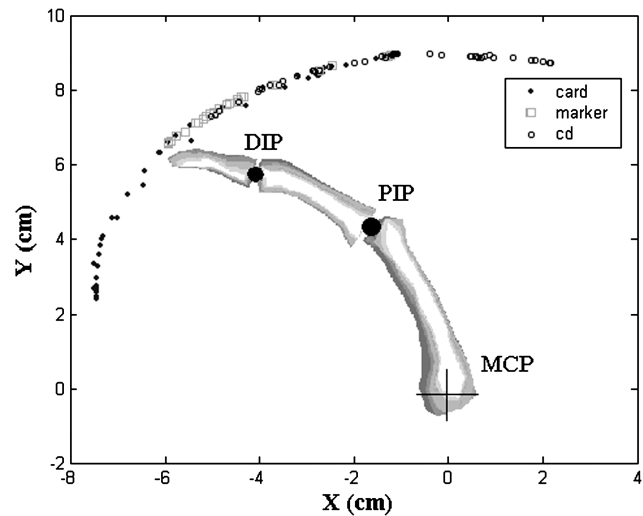


FIG. 2. Trajectory of tip of index finger in the x-y plane for 3 different trials: grasping the marker, the CD, or the playing card. Origin of the coordinate system (0,0) is located at the center of the metacarpophalangeal (MCP) joint. The y axis is aligned with the 1st metacarpal, while the x axis is perpendicular to the palm. Thus negative x values denote movements of the fingertip on the palmar side of the hand. Actual finger posture is shown for a particular point along the trajectory.

contact with the object. On receiving a verbal cue, the subject released the object and moved his/her arm either to the next object or back to the starting position.

Each subject performed all trials with her/his dominant hand. Thus nine subjects used their right hands, and one subject used his left hand. Finger joint angles were recorded at 50 Hz throughout the trials with a CyberGlove (Immersion Corp., San Jose, CA). Specifically, the flexion/extension of the distal interphalangeal (DIP), proximal interphalangeal, (PIP), and metacarpophalangeal (MCP) joints were recorded for the fingers, along with MCP abduction/adduction. Thumb carpometacarpal (CMC) abduction/adduction and flexion/extension were also measured, along with thumb MCP and interphalangeal (IP) flexion/extension.

After completion of the trials, the length of each digit segment (distal, middle, proximal, and thumb metacarpal) was measured with

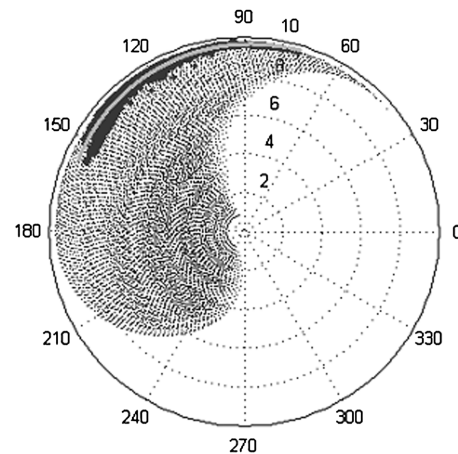


FIG. 3. Example of the index fingertip location across all 20 trials for 1 subject. Data are plotted in polar coordinates, with the concentric circles indicating loci of equal length r (cm) and the straight lines indicating loci of equal angle theta. MCP joint is centered at r = 0, with theta = 90° corresponding to the neutral position. Lighter dots represent the extent of the potential workspace in which the fingertip could move. Darker dots represent the actual fingertip locations. Solid line represents the spiral fit to data (mean error = 0.1 cm).

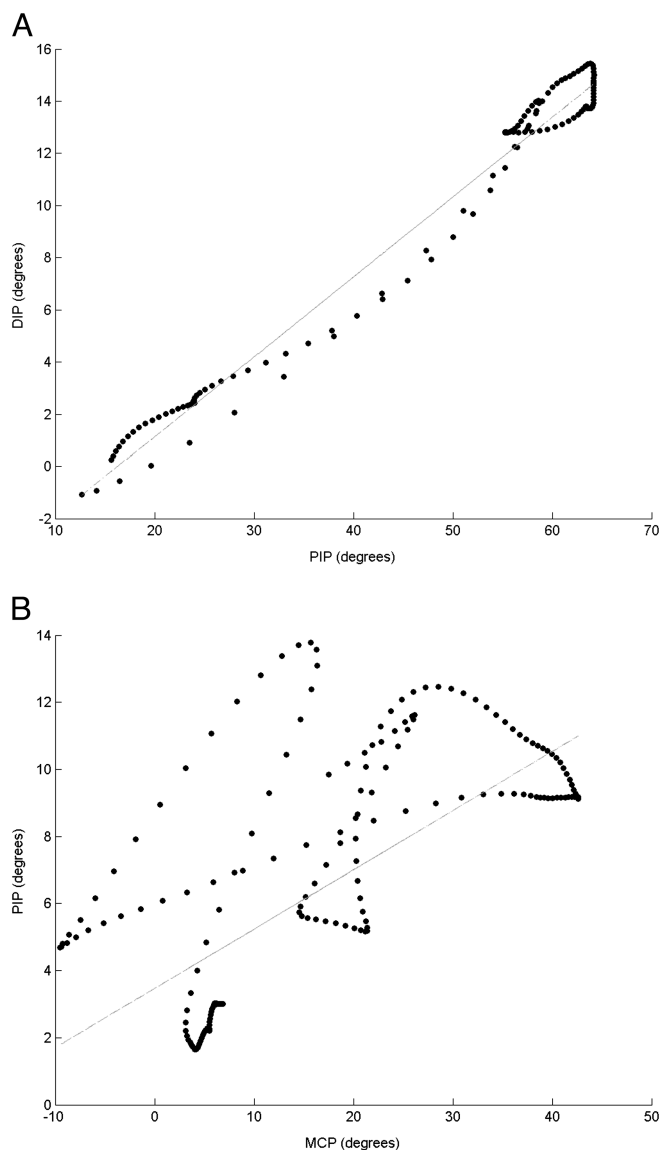


FIG. 4. Examples of relations between joints on the same finger for a given trial. For these specific trials, linear regression fit the proximal interphalangeal (PIP)-distal interphalangeal (DIP) data well in A ($R^2 = 0.98$), but not the MCP-PIP data in B ($R^2 = 0.50$). Positive angles denote joint flexion.

digital calipers. For the more proximal segments, the distance was taken from joint-center to joint-center. For the distal segments, the measurement was made from the joint-center to the fingertip. These data were saved and used to compute fingertip path and workspace values.

Five of these subjects participated in a further experiment during a separate testing session. This experiment was designed to test for the possible influence of initial finger posture on finger trajectory. The subjects completed the same protocol as described but with initial and final posture consisting of a closed fist.

Calibration

Calibration was performed at each joint of interest. Prior to performance of the trials, data were recorded at multiple known joint angles (measured with a finger goniometer (Pluri-Dig, Sammons Preston, Chicago, IL). Calibration curves were formulated from this data for each joint by creating a polynomial function relating known joint angle to voltage measured by the CyberGlove sensors.

All data subsequently acquired during the testing session were digitally filtered forward and backward with a 20th-order finite impulse response having a cut-off frequency of 5 Hz, a value similar to that used in other studies (Mason et al. 2001). Examination of the power spectral density of the raw data confirmed that the power of the signal resided predominantly below 5 Hz. The data were calibrated according to the aforementioned functions.

Data analysis

The potential for linear relationships between joints for a given finger was assessed using linear regression. For each finger, the best fit for a line relating PIP joint angle to MCP joint angle was found using the least-squares error for each trial. In like manner, a line was fit to the DIP versus PIP joint angle data for each subject for each trial. To reduce spurious weighting, the portions of the trial at the beginning and end when neither joint angle was changing were first removed from the record. The beginning of the active portion of the trial was defined by the point at which the absolute difference between joint angle, averaged across a 60-ms moving window, and initial angle first exceeded 0.5° . The end of the active portion of the trial was defined as the last point at which the absolute difference between the actual and final joint angles exceeded 0.5° .

The slope and coefficient of the linear relationship between the two joint angles were computed using linear regression. R^2 values were computed for each regression to provide an estimate of the fit. The R^2 and slope values were averaged across all trials for each subject. These values for the PIP-MCP relationship were compared with those of the DIP-PIP relationship across subjects using a repeated measures ANOVA, with finger and joint pair serving as the independent variables.

Relationships between angular movements for the same joint in different fingers were also examined. Correlation matrices were computed for the MCP, PIP, and DIP joints. A mean value for each element in the matrices was computed across all subjects.

Locations of the tips of the digits were computed from the joint angle data and segment lengths using forward kinematics. For the four fingers, fingertip location was computed with respect to a base coordinate system located on the MCP joint for each finger. Thus fingertips were always located within a plane coincident with the sagittal plane of the phalanges. Coordinate systems were assigned to the finger segments at each of the finger joints, with the z axis aligned with the joint of rotation, characterizing MCP extension/flexion (θ_1), PIP extension/flexion (θ_2), and DIP extension/flexion (θ_3). The y axis pointed from the proximal to distal coordinate system, while the x axis was directed dorsally (Buchholz and Armstrong 1992). All of the y axes were aligned when the joints were in the neutral position. Thus fingertip location could be described by

$$\begin{aligned} x &= l_{DP} * \sin(\theta_1 + \theta_2 + \theta_3) + l_{MP} * \sin(\theta_1 + \theta_2) + l_{PP} * \sin(\theta_1) \\ y &= l_{DP} * \cos(\theta_1 + \theta_2 + \theta_3) + l_{MP} * \cos(\theta_1 + \theta_2) + l_{PP} * \cos(\theta_1) \end{aligned} \quad (1)$$

where l_{DP} , l_{MP} , and l_{PP} represent the lengths of the distal, middle, and proximal finger segments, respectively. The description of the fingertip location was also transformed from the Cartesian coordinate sys-

TABLE 2. Mean outcomes for regression assessment of joint relationships

Finger	PIP-MCP		DIP-PIP	
	Slope	R^2	Slope	R^2
Index	0.26	0.31	0.32	0.65
Middle	0.37	0.36	0.36	0.71
Ring	0.72	0.46	0.16	0.51
Little	0.70	0.47	0.25	0.59

TABLE 3. Coefficients of correlation between joint rotations for different fingers

	MCP				PIP				DIP			
	I	M	R	L	I	M	R	L	I	M	R	L
I	1	0.92	0.82	0.44	1	0.82	0.72	0.64	1	0.53	0.34	0.34
M	0.92	1	0.93	0.53	0.82	1	0.83	0.76	0.53	1	0.63	0.54
R	0.82	0.93	1	0.61	0.72	0.83	1	0.85	0.34	0.63	1	0.46
L	0.44	0.53	0.61	1	0.64	0.76	0.85	1	0.34	0.54	0.46	1

tem into a polar coordinate system for analysis. Distance from the MCP joint was given by the variable r , while the direction of the vector pointing from the MCP to the fingertip was described by the angle θ . When the fingertip is aligned with the metacarpal bone, $\theta = 90^\circ$.

A variety of curves were fit to the fingertip trajectory data to be used in quantifying how stereotypical the trajectories were. Data from all of the trials were pooled for each subject. From inspection, it was decided to try to fit the data with either a second-order polynomial in the x - y plane (Eq. 2) or a logarithmic spiral in the θ - r plane (Eq. 3). The polynomial coefficients were determined from multiple regression by least-squares estimation. The spiral coefficients were obtained using a nonlinear least-squares estimation with a Levenberg-Marquardt search algorithm

$$y = ax^2 + bx + c \tag{2}$$

$$r = ae^{b\cot\theta} \tag{3}$$

Goodness of fit was quantified by computing the absolute error between the dependent value estimated from the function (\hat{y} or \hat{r}) and the actual value from the data (y or r). The average and SD of the absolute error were computed for each subject. Absolute errors of the logarithmic spiral and polynomial fits were compared using a paired t -test. The errors for the different fingers were compared using a repeated measures ANOVA. Variance accounted for (VAF) was also computed to determine the fit of the estimated \hat{x} and \hat{y} values, calculated from the \hat{r} , to the actual x - y fingertip locations (Perreault et al. 1999).

For the subjects completing the second experiment, data from the 10 grasping trials for multiple objects were pooled to quantify voluntary fingertip trajectory. We excluded all data in which fingertip trajectory was constrained due to requirements to begin or end in a fistful posture. Thus the data from the single object trials were not used for estimating the trajectory. Only the data occurring between the grasp of the first object and the release of the fifth object in the multi-object trials were used.

Temporal movement properties were also assessed, both in terms of position and velocity. These data were examined in Cartesian space, where it was most readily visualized. Since the x and y positions were related, as described above, we focused our analysis on only the x position data. We computed the number of peaks in the x position curve plotted versus time during an entire trial. The x position data were searched for local minima and maxima. An absolute difference in position between adjacent extrema greater than a threshold value signified a peak. A relatively conservative threshold value of 20% of the range of x during a given trial was arbitrarily chosen (Kamper et al. 2002b). A repeated measures ANOVA was performed on these data to determine if object shape/size affected the temporal pattern of hand opening and closing.

Movement velocity was quantified by examining the tangential velocity. We determined the number of peaks that appeared during the entire trial in the speed curve, given by the norm of the tangential velocity. An absolute difference in speed between consecutive extrema greater than a threshold value signified a peak. A threshold value equal to 20% of the peak tangential speed for a given trial was employed.

Location of the tip of the thumb was computed in three-dimensional Cartesian space for a coordinate system attached to the carpal side of the CMC joint. The z axis for this coordinate system is parallel to those of the finger base coordinate systems. Seven coordinate transformations were used to convert location of the tip of the thumb (${}^E\mathbf{p}_E$) to the base coordinate system (${}^0\mathbf{p}_E$; Eq. 4). The homogeneous transformations (\mathbf{T}) correspond to CMC axial rotation (θ_1), followed by CMC abduction (θ_2), followed by CMC flexion (θ_3), followed by MCP axial rotation (θ_4), followed by MCP flexion (θ_5), followed by IP flexion (θ_6), followed by translation from the IP joint to the tip of the thumb (Giurintano et al. 1995; Imaeda et al. 1996). CMC axial rotation (θ_1) was fixed to be a constant value of 45° . This was estimated by measuring the angle of the plane containing the thumb, with the MP and IP joints at zero flexion, to the plane containing the fingers with the MCP, PIP, and DIP joints at zero flexion. Similarly, measurements on subjects led us to compute MCP axial rotation (θ_4) as a linear function of CMC flexion (see APPENDIX A). Namely, we set $\theta_4 = 0.4 \times \theta_3$

$${}^0\mathbf{p}_E = \begin{bmatrix} p_x \\ p_y \\ p_z \\ 1 \end{bmatrix}, \quad {}^0\mathbf{p}_E = {}^0\mathbf{T}_1 {}^1\mathbf{T}_2 {}^2\mathbf{T}_3 {}^3\mathbf{T}_4 {}^4\mathbf{T}_5 {}^5\mathbf{T}_6 {}^E\mathbf{p}_E \tag{4}$$

The potential thumb workspace for each subject was computed by allowing the joint angles to span their ranges of motion, with peak CMC flexion set to be a function of CMC abduction. The resulting locations of the tip of the thumb were found through forward kinematics (Eq. 4). The volume of this workspace was computed by finding the convex hull for the space. The convex hull, Delaunay triangulation (division of the hull surface into a set of triangles with the smallest possible total edge length), and volume encompassed by

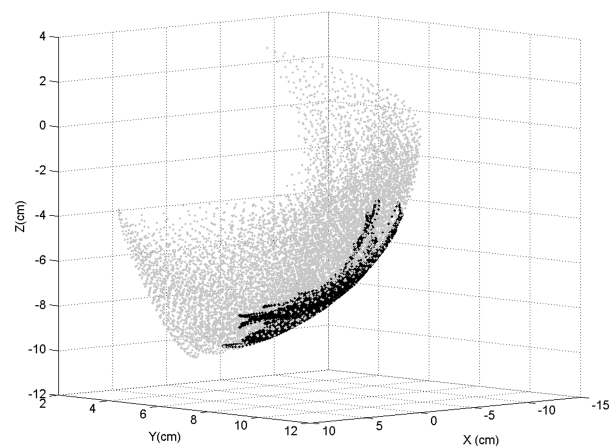


FIG. 5. Potential workspace (lighter dots) for 1 subject and the part of the workspace actually used (darker dots) during the 20 grasping trials. x - y - z location of the tip of the thumb is shown with respect to the coordinate system fixed to the hand at the carpometacarpal (CMC) joint. z axis is directed out from the hand, y axis is parallel to hand, and x axis lies within plane of hand, directed from the index toward the little finger. Thumb trajectories resided primarily on the surface of the workspace, such that the utilized volume represented only 4.2% of the total for this subject.

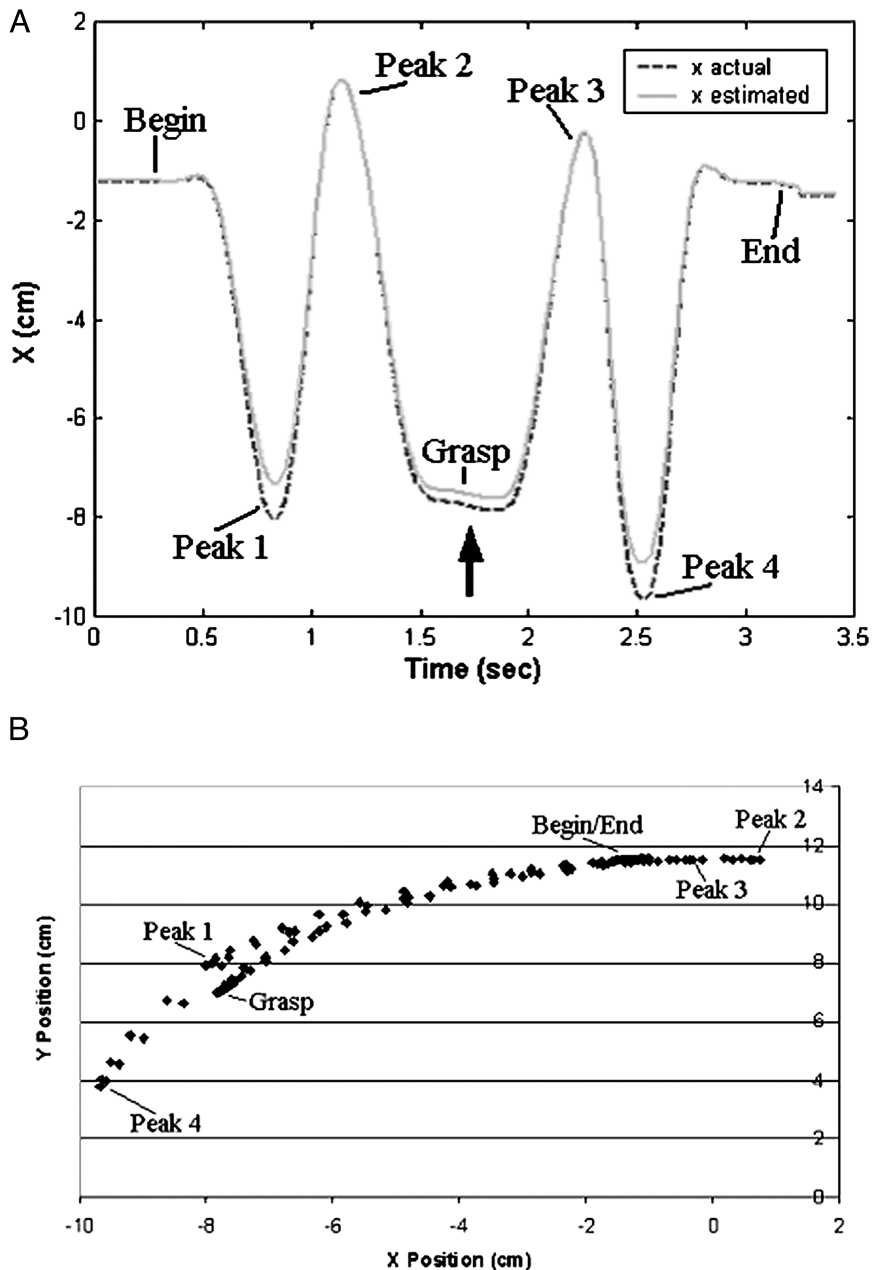


FIG. 6. A: temporal portrait of movement of the middle fingertip in the x direction for a single trial of grasping the softball. Actual data (dashed line) and fit data (solid line) are shown. Heavy arrow indicates middle portion of the contact period with the ball. B: corresponding fingertip location in the x - y plane, demarcating the locations of the points marked in A.

the convex hull were computed with MATLAB using the QuickHull Algorithm (Barber et al. 1996). Because the planar projection of the space was crescent-shaped, convex hulls were fit to both the inner and outer surfaces comprising the thumb workspace (Fig. 1). Subtraction of the volume encompassed by the inner hull from the volume encompassed by the outer hull yielded the workspace volume. Volume of the thumb workspace actually spanned during the trials was computed in a similar fashion. This volume was expressed as a percentage of the theoretical workspace volume.

RESULTS

Ten subjects participated in grasping trials of five different objects. Subjects were instructed to begin and finish the trials with the hand resting comfortably on the leg. This resulted in an extended finger position. Joint angles were fairly uniform even across subjects (Table 1). Trial-to-trial variability in start-

ing hand posture for a single subject was slightly smaller than the values shown in Table 1.

For a given subject, finger trajectories were quite consistent across trials. These trajectories were curved rather than straight in the plane of the finger. Subjects tended to move along different portions of a specific trajectory for differently sized objects rather than to create new trajectories (Fig. 2).

The logarithmic spiral (Fig. 3) provided a better fit to the data than the polynomial, as determined by the size of the absolute error (0.22 ± 0.25 vs. 0.51 ± 0.61 cm, $P < 0.01$). For the spiral, mean error for each finger from the spiral trajectory was always < 0.5 cm, except for one finger for one subject. This subject displayed a fairly consistent pattern for the little finger, but one that was unique and involved curling of the finger. Across all subjects, the mean error for different fingers was only marginally significant ($P = 0.1$), with mean error

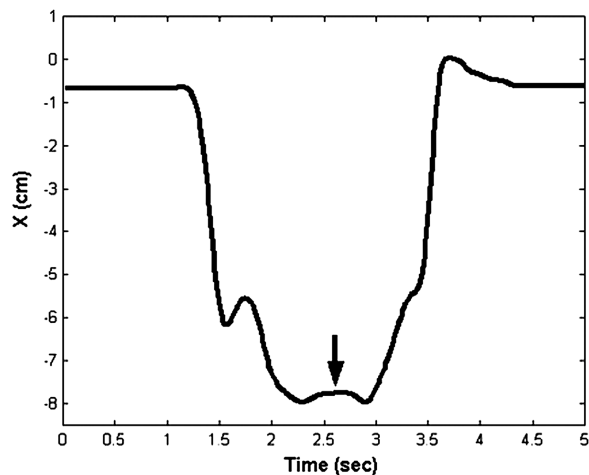


FIG. 7. Temporal portrait of movement in the x direction for the single trial of grasping the marker (same subject and finger shown in Fig. 4). Arrow is centered on portion of trial during which subject grasped marker. Release phase exhibits a monotonic increase in x .

from the spiral tending to be smaller for the index and ring fingers (0.20 cm) than for the middle finger (0.27 cm). Mean VAF across all trials and subjects was $>98\%$ for both the x and y directions. The estimated x and y positions matched the experimental data quite well (Fig. 6).

A variety of grasping strategies was used among subjects and among objects. For example, some subjects used the thumb and two digits to grasp the softball while others used all five digits. Some subjects supinated the forearm to grasp the playing card with a palmar pinch, some pronated the forearm, and others kept the forearm somewhere between the two extremes and grasped the opposing edges of the card. However, the spiral shape of the trajectories was quite consistent, as quantified by the β coefficient (Eq. 3), which had a value across all fingers of 1.66 ± 0.05 radians. This β term controls the rate of decay of the spiral. Because it is significantly greater than $\pi/2$, the finger is not merely sweeping along a circular arc. This assertion is further supported by the fact that the mean error of the spiral fit was always less than that for an arc of constant radius.

Five subjects completed the second experiment with finger posture starting and ending in a fist. Mean starting finger posture was 50° of MCP flexion, 100° of PIP flexion, and 45° of DIP flexion. For these subjects, a similar spiral pattern was also observed for the portions of the trials not constrained by the fist posture, i.e., the portion between the grasp of the first object and release of the fifth object in the multi-object trials. For a spiral fit to this pooled data, mean VAF in both the x and y directions was again $>98\%$. The pattern closely matched that observed during the previous session. In fact, using the coefficient estimates from the first experiment to predict x and y positions for the second experiment led to mean VAF = 95% for both directions.

Relationships between joint angles for a given finger were considerably more variable than the fingertip trajectories. While highly linear relationships between consecutive joint angles could sometimes be found ($R^2 > 0.9$), for many other trials, this was not the case (see Fig. 4B). Significant variation could be observed even between consecutive trials with the same object. Overall, the linear relationship better defined the

PIP-DIP correspondence ($R^2 = 0.61$ across all fingers) than the MCP-PIP correspondence ($R^2 = 0.40$ across all fingers; $P = 0.001$). The repeated measures ANOVA for the slope indicated a significant interaction between finger and joint pair ($P = 0.001$), with the slope of the PIP-MCP relationship being significantly larger than the slope of the DIP-PIP relationship for the ring and little fingers (Table 2). All of the slopes are less than one, thereby indicating that MCP flexion was greater than PIP flexion, which was, in turn, greater than DIP flexion.

Between fingers, the correlations between corresponding joints were significant. These correlations were greatest for adjacent fingers, and for the MCP joints (Table 3). Comparison of the relationships between pairs of joints within and across fingers can be made by squaring the coefficients of correlation in Table 3 to obtain the coefficients of determination, similar to the R^2 values in Table 2. Especially for the MCP and PIP joints, correlations between fingers are much greater than those within a finger.

Thumb motion tended to vary more according to object size/shape. The volume traversed, however, was still quite selective. Across all 20 trials, subjects used $3.6 \pm 1.3\%$ of their potential workspace. The majority of the movement occurred near the surface of the potential workspace (Fig. 5).

The temporal finger pattern generally did not exhibit a monotonic change between initial and final posture, especially for the x direction. For the single-object trials in which subjects had an extended initial hand posture, multiple peaks in the temporal curves were typically present, indicating hand closure during the transport phase (Fig. 6). The pattern was similar for grasp and release. The x position data had 4.4 ± 1.6 peaks for each trial.

The temporal pattern was dependent on object size/shape. For the smaller diameter objects such as the marker, the hand closure could sometimes be incorporated into the object grasp so that little or no change in direction occurred (Fig. 7). The numbers of peaks in the x position curves for the card (3.3) and marker (3.2) were statistically different from the number of peaks for the ball (5.0), CD (5.3), and cup (5.4; $P < 0.001$).

For the trials begun with a closed fist, the temporal x position curve looked similar to that obtained with an initially extended finger posture (Fig. 8). The initial decrease in the x position

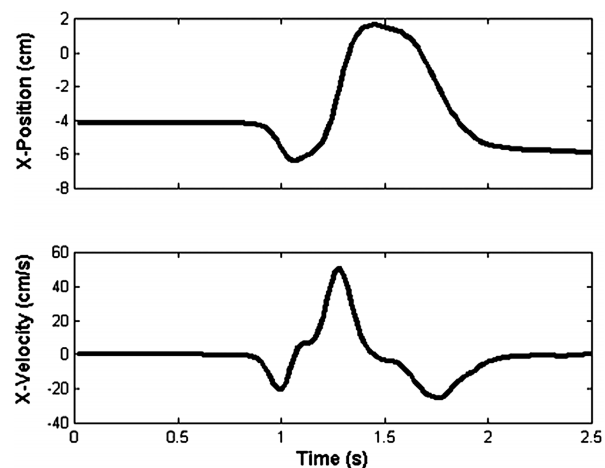


FIG. 8. Temporal record for a motion from a fist to grasp of a cup. Velocity signal was computed from the position signal using a 5-point difference formula. Subject contacted the cup at approximately 2.2 s.

was due in this case, however, to the fingers following a curved rather than straight trajectory during hand opening. The corresponding velocity curve, obtained by numerical differentiation of the position curve, displayed multiple peaks and three zero-crossings after the start of movement.

The tangential velocity profiles also displayed multiple peaks (Fig. 9). Across single-object trials for the 10 subjects, the mean number of speed peaks (NSP) was 5.0 ± 1.5 . In accordance with the described temporal movement patterns, NSP was greater for the larger diameter objects, such as the cup, than for smaller diameter objects, such as the marker ($P < 0.001$).

DISCUSSION

For reach-to-grasp movements to a variety of objects, fingertip motion was quite similar. The movement tended to follow a particular curved path, described well by a logarithmic spiral. Object size affected finger motion largely in terms of distance covered along the spiral, which was located near the outer edge of the fingertip workspace. These trajectories were quite consistent, independent of the starting finger posture, whether extended or actively flexed into a fist. In essence, the spiral trajectory served as an attractor in dynamics parlance, as described in rhythmic finger movements (Kay et al. 1991).

In accordance with another study, thumb movement was more variable than finger motion, with a greater dependency on object shape and size (Smeets and Brenner 2001). The percentage of the available workspace used, however, was still quite small. Flexion of the MP and IP joints was limited, as seen elsewhere (Santello et al. 2002), thereby leaving most of the thumb trajectories to reside on the surface of the workspace.

The consistency of the movements corresponds well to other studies having displayed highly repeatable movement paths for the hand during reaching (Wolpert et al. 1995). However, unlike the hand trajectories in planar movements (Shadmehr and Mussa-Ivaldi 1994), fingertip trajectories are curved. These trajectories thus do not follow the straight-line trajectory predicted by the minimum jerk hypothesis (Flash and Hogan 1985) and postulated as the preferred finger pathway (Secco and Magenes 2002).

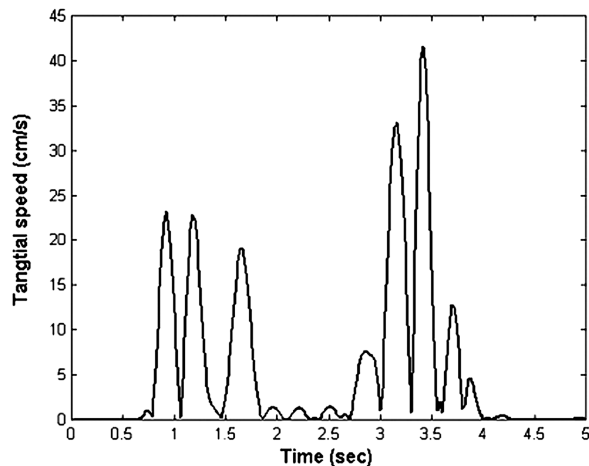


FIG. 9. Tangential speed of the fingertip trajectory for the ring finger during a single trial of grasping the softball (number of speed peaks=6). The relatively quiescent period from 1.8 to 2.7 s was the portion of the trial the subject was in contact with the ball.

Smeets and Brenner (1999) did show how minimum jerk theory could still predict a curved path without via points. A nonzero boundary condition on the acceleration at the time of contact with the target could produce curved finger trajectories that were still minimum jerk. For our results, however, such as those seen in Figs. 6 and 8, a minimum jerk solution is not possible. Three roots for the x velocity are seen after initiation of movement (Fig. 8), and only two are possible for the minimum jerk solution (APPENDIX B).

Certainly, curved motion pathways have been observed in a number of other experimental paradigms. Unconstrained planar reaching resulted in significantly greater hand path curvature than planar reaching in which interaction with an external object was required (Desmurget et al. 1997). The curvature also increased with increasing angle of the target from the midline, a phenomenon also seen in unconstrained three-dimensional reaching (Kamper et al. 2002b).

The observed spatial pattern of movement does require a coordinated effort of a number of different muscles. For example, excitation of the intrinsic muscles alone, resulting in MCP flexion with PIP and DIP extension, is insufficient to generate the observed patterns. PIP and DIP flexion were significant during the grasping, as evidenced by the spiral fit (Fig. 4A). Alternatively, stimulation of only the extrinsic finger flexors, flexor digitorum superficialis and profundus, produces a very different pattern of movement than the one seen, with the greatest rotation occurring at the PIP joint (Kamper et al. 2002a). Electromyographic studies of finger movement have verified the large percentage of finger muscles active for even a relatively simple movement (Brandell 1970; Rose et al. 1999).

Governing principles for the spatial patterns of finger movement remain elusive. As correlations for movements between pairs of joints varied widely, synergistic planning of movement in joint space (Desmurget et al. 1995; Gandolfo et al. 1996; Soechting and Lacquaniti 1981) does not seem to provide a plausible alternative. Incidentally, the slope value of 0.3 that we obtained for the PIP-DIP relationship was actually less than one-half of that described by others (Hahn et al. 1995), but the tasks were different. Where our tasks entailed grasping and releasing objects, the task in that study was to open and close the fist, an exercise requiring much greater PIP and DIP flexion. It is also possible that the CyberGlove itself altered DIP movement by providing resistance to DIP flexion.

For a given type of joint (MCP, PIP, DIP), movement in one finger was closely correlated with that in adjacent fingers. The correlation between joints of the same type on different fingers was greater than the correlation between joints of different type on the same finger (Tables 2 and 3). This phenomenon was also observed in studies with a greater variety of objects (Santello et al. 2002), although objects with nonuniform diameters may preclude its occurrence (Santello and Soechting 1998). The high correlations between pairs of fingers seem to result from neural rather than mechanical constraints, in accordance with studies describing neural enslaving of fingers during isometric force generation (Latash et al. 2002a; Zatsiorsky et al. 1998). Indeed, anatomical studies in primates have detected motor units that exert tension on multiple finger tendons (Schieber et al. 1997).

Possibly, the observed fingertip trajectories represent the paths of minimal resistance against passive torques, which

appear to fundamentally affect finger motion (Kamper et al. 2002a). It is intriguing that even from an initial fist ed posture, the finger trajectories largely returned to the pathways obtained with an initially relaxed hand.

Temporal fingertip motion was affected by object size/shape. Whether or not appropriate for object grasp, the hand began to close during transport to the object, as described elsewhere (Hoff and Arbib 1993). For objects of a particular shape, especially those with a smaller diameter, this motion would sometimes segue into hand closure for grasp, without an interceding overshoot in hand opening. For the larger diameter objects, however, hand closure during transport was typically followed by hand opening and then hand closing for grasp, with a reversal of this sequence for release and hand transport to a new position. This is very similar to what was observed in other studies when subjects were instructed to begin reach-to-grasp tasks with the fingers extended rather than in contact with the thumb (Saling et al. 1996; Timmann et al. 1996). These temporal patterns may result from interdependence between reaching and grasping (Haggard and Wing 1995). Alternatively, the initial hand closing could be produced by passive joint mechanics.

Certainly, the human hand is capable of exploring and working throughout its physically available workspace. When required, vastly different digit trajectories than the ones observed in this study can be produced. However, for a variety of grasping tasks, specific trajectories covering a small portion of the workspace are routinely employed by healthy individuals. This suggests that, following impairment of the hand, return of control over even this small percentage of the workspace through rehabilitation or external assistance could lead to considerable improvement in function. Restoration of the active range of motion of the MCP and CMC joints appears most critical for production of the grasping motions used in this study.

APPENDIX A

Homogeneous transform matrices

$${}^0T_1 = \begin{bmatrix} \cos(D * \theta_1) & -\sin(D * \theta_1) & 0 & 0 \\ 0 & 0 & 1 & 0 \\ -\sin(D * \theta_1) & -\cos(D * \theta_1) & 0 & 0 \\ 0 & 0 & 0 & 1 \end{bmatrix}$$

$${}^1T_2 = \begin{bmatrix} \cos(D * \theta_2) & -\sin(D * \theta_2) & 0 & 0 \\ 0 & 0 & -1 & 0 \\ \sin(D * \theta_2) & \cos(D * \theta_2) & 0 & 0 \\ 0 & 0 & 0 & 1 \end{bmatrix}$$

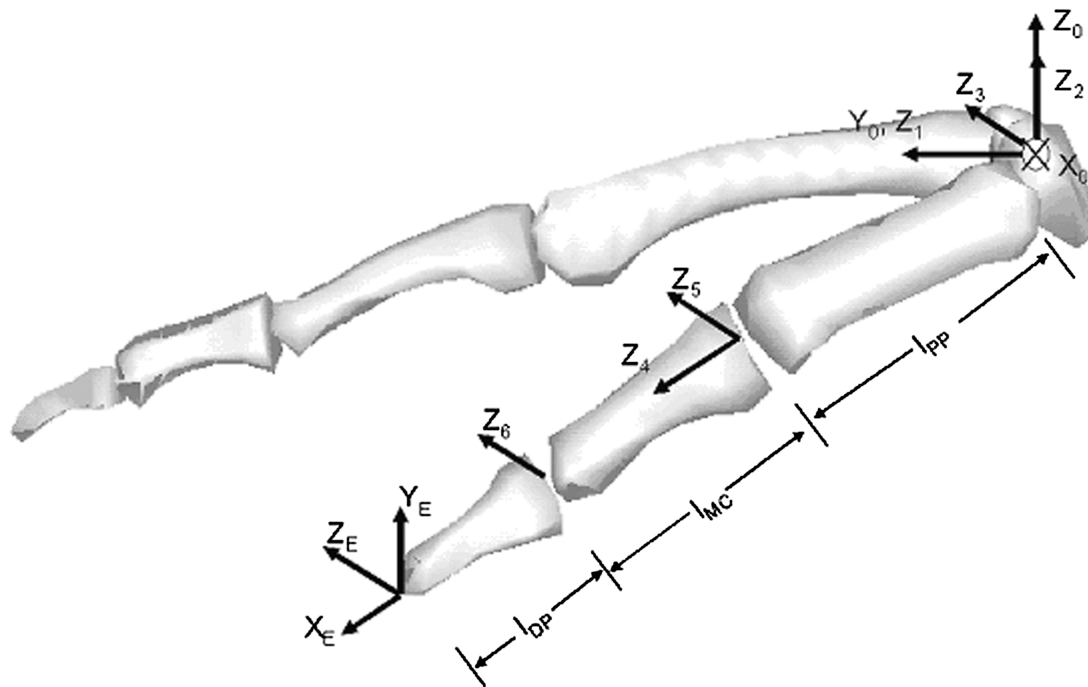
$${}^2T_3 = \begin{bmatrix} 0 & 0 & 1 & 0 \\ \cos(\theta_3) & -\sin(\theta_3) & 0 & 0 \\ \sin(\theta_3) & \cos(\theta_3) & 0 & 0 \\ 0 & 0 & 0 & 1 \end{bmatrix}$$

$${}^3T_4 = \begin{bmatrix} 0 & 0 & 1 & l_{MC} \\ -\sin(D * \theta_4) & -\cos(D * \theta_4) & 0 & 0 \\ \cos(D * \theta_4) & -\sin(D * \theta_4) & 0 & 0 \\ 0 & 0 & 0 & 1 \end{bmatrix}$$

$${}^4T_5 = \begin{bmatrix} 0 & 0 & 1 & 0 \\ -\sin(\theta_5) & -\cos(\theta_5) & 0 & 0 \\ \cos(\theta_5) & -\sin(\theta_5) & 0 & 0 \\ 0 & 0 & 0 & 1 \end{bmatrix}$$

$${}^5T_6 = \begin{bmatrix} \cos(\theta_6) & -\sin(\theta_6) & 0 & l_{PP} \\ \sin(\theta_6) & \cos(\theta_6) & 0 & 0 \\ 0 & 0 & 1 & 0 \\ 0 & 0 & 0 & 1 \end{bmatrix}$$

$${}^6T_E = \begin{bmatrix} 1 & 0 & 0 & l_{DP} \\ 0 & 1 & 0 & 0 \\ 0 & 0 & 1 & 0 \\ 0 & 0 & 0 & 1 \end{bmatrix} \quad \begin{matrix} \theta_1 = 45^\circ \\ \theta_4 = 0.4 * \theta_3 \\ D = \begin{cases} 1, \text{ left hand} \\ -1, \text{ right hand} \end{cases} \end{matrix}$$



APPENDIX B

A minimum jerk solution for a movement in the x - y plane is given by the following equations (Flash and Hogan 1985)

$$\begin{aligned}x &= a_5t^5 + a_4t^4 + a_3t^3 + a_2t^2 + a_1t + a_0 \\y &= a_5t^5 + a_4t^4 + a_3t^3 + a_2t^2 + a_1t + a_0\end{aligned}\quad (5)$$

The polynomial coefficients are determined by the boundary conditions. For our movements, in which the fingers are initially at rest, the initial boundary conditions for x are given by [$x(0) = x_0$, $\dot{x}(0) = 0$, $\ddot{x}(0) = 0$]. Arbitrarily setting $x_0 = 0$, yields

$$x = a_5t^5 + a_4t^4 + a_3t^3 \quad (6)$$

Thus the velocity is given by

$$\dot{x} = 5a_5t^4 + 4a_4t^3 + 3a_3t^2 \quad (7)$$

The velocity \dot{x} thus has only two roots for $t \neq 0$, irrespective of the final boundary conditions. To match Fig. 6, three roots are needed after the starting time $t = 0$.

Figure 1 was generated with software written at the Geometry Center, University of Minnesota.

DISCLOSURES

This work was supported by grants from the Whitaker Foundation, the Women's Board of the Rehabilitation Institute of Chicago, and the National Institute of Child Health and Human Development Training Grant T32 HD-07418.

REFERENCES

- Barber CB, Dobkin DP, and Huhdanpaa H.** The Quickhull Algorithm for convex hulls. *ACM Trans Mathematical Software* 22: 469–483, 1996.
- Brandell BR.** An electromyographic-cinematographic study of the muscles of the index finger. *Arch Phys Med Rehabil* 51: 278–285, 1970.
- Buchholz B and Armstrong TJ.** A kinematic model of the human hand to evaluate its prehensile capabilities. *J Biomech* 25: 149–162, 1992.
- Cruse H, Wischmeyer E, Brüwer M, Brockfield P, and Dress A.** On the cost functions for the control of the human arm movement. *Biol Cybern* 62: 519–528, 1990.
- Desmurget M, Jordan M, Prablanc C, and Jeannerod M.** Constrained and unconstrained movement involve different control strategies. *J Neurophysiol* 77: 1644–1650, 1997.
- Desmurget M, Prablanc C, Arzi M, Rossetti Y, Paulignan Y, Urquizar C, and Mignot JC.** Postural and synergic control for three-dimensional movements of reaching and grasping. *J Neurophysiol* 74: 905–910, 1995.
- Engelbrecht SE.** Minimum principles in motor control. *J Math Psychol* 45: 497–542, 2001.
- Flash T and Hogan N.** The coordination of arm movements: an experimentally confirmed mathematical model. *J Neurosci* 5: 1688–1703, 1985.
- Gandolfo F, Mussa-Ivaldi FA, and Bizzi E.** Motor learning by field approximation. *Proc Natl Acad Sci USA* 93: 3843–3846, 1996.
- Gentilucci M, Chieffi S, Scarpa M, and Castiello U.** Temporal coupling between transport and grasp components during prehension movement: effects of visual perturbation. *Exp Brain Res* 47: 71–82, 1992.
- Giurintano DJ, Hollister AM, Buford WL, Thompson DE, and Myers LM.** A virtual five-link model of the thumb. *Med Eng Phys* 17: 297–303, 1995.
- Haggard P and Wing A.** Coordinated responses following mechanical perturbation of the arm during prehension. *Exp Brain Res* 102: 483–494, 1995.
- Hahn P, Krimmer H, Hradetzky A, and Lanz U.** Quantitative analysis of the linkage between the interphalangeal joints of the index finger: an in vivo study. *J Hand Surg [Br]* 20B: 696–699, 1995.
- Hoff B and Arbib MA.** Models of trajectory formation and temporal interaction of reach and grasp. *J Motor Behav* 25: 175–192, 1993.
- Imaeda T, Cooney WP, Niebur GL, Linscheid RL, and An K.** Kinematics of the trapeziometacarpal joint: a biomechanical analysis comparing tendon interposition arthroplasty and total-joint arthroplasty. *J Hand Surg* 21A: 544–553, 1996.
- Jeannerod M.** The timing of natural prehension movements. *J Motor Behav* 16: 235–254, 1984.
- Kamper DG, Hornby TG, and Rymer WZ.** Extrinsic flexor muscles generate concurrent flexion of all three finger joints. *J Biomech* 35: 1581–1589, 2002a.
- Kamper DG, McKenna-Cole AN, Kahn LE, and Reinkensmeyer DJ.** Alterations in reaching after stroke and their relation to movement direction and impairment severity. *Arch Phys Med Rehabil* 83: 702–707, 2002b.
- Kay BA, Saltzman EL, and Kelso JA.** Steady-state and perturbed rhythmic movements: a dynamical analysis. *J Exp Psychol Hum Percept Perform* 17: 183–197, 1991.
- Latash ML, Li S, Danion F, and Zatsiorsky VM.** Central mechanisms of finger interaction during one- and two-hand force production at distal and proximal phalanges. *Brain Res* 924: 198–208, 2002a.
- Latash ML, Scholz JF, Danion F, and Schoner G.** Finger coordination during discrete and oscillatory force production tasks. *Exp Brain Res* 146: 419–432, 2002b.
- Li Z, Latash ML, and Zatsiorsky VM.** Force sharing among fingers as a model of the redundancy problem. *Exp Brain Res* 119: 276–286, 1998.
- Mason CR, Gomez JE, and Ebner TJ.** Hand synergies during reach-to-grasp. *J Neurophysiol* 86: 2896–2910, 2001.
- Morasso P.** Spatial control of arm movements. *Exp Brain Res* 42: 223–227, 1981.
- Perreault EJ, Kirsch RF, and Acosta AM.** Multiple-input, multiple-output system identification for characterization of limb stiffness dynamics. *Biol Cybern* 80: 327–337, 1999.
- Rose CR, Keen DA, Koshland GF, and Fuglevand A.** Coordination of multiple muscles in the elaboration of individual finger movements. *Soc Neurosci Abstr* 25: 466.6, 1999.
- Saling M, Mescheriakov S, Molokanova E, Stelmach GE, and Berger M.** Grip reorganization during wrist transport: the influence of an altered aperture. *Exp Brain Res* 108: 493–500, 1996.
- Santello M, Flanders M, and Soechting JF.** Patterns of hand motion during grasping and the influence of sensory guidance. *J Neurosci* 22: 1426–1435, 2002.
- Santello M and Soechting JF.** Gradual molding of the hand to object contours. *J Neurophysiol* 79: 1307–1320, 1998.
- Schieber MH, Chua M, Petit J, and Hunt CC.** Tension distribution of single motor units in multitendoned muscles: comparison of a homologous digit muscle in cats and monkeys. *J Neurosci* 17: 1734–1747, 1997.
- Secco EL and Magesen G.** A feedforward neural network controlling the movement of a 3-DOF finger. *IEEE Trans Sys Man Cybern* 32: 437–445, 2002.
- Shadmehr R and Mussa-Ivaldi FA.** Adaptive representation of dynamics during learning of a motor task. *J Neurosci* 14: 3208–3224, 1994.
- Smeets JBJ and Brenner E.** A new view on grasping. *Motor Control* 3: 237–271, 1999.
- Smeets JBJ and Brenner E.** Independent movements of the digits in grasping. *Exp Brain Res* 139: 92–100, 2001.
- Soechting JF and Flanders M.** Flexibility and repeatability of finger movements during typing: analysis of multiple degrees of freedom. *J Comput Neurosci* 4: 29–46, 1997.
- Soechting JF and Lacquaniti F.** Invariant characteristics of a pointing movement in man. *J Neurosci* 1: 710–720, 1981.
- Timmann D, Stelmach GE, and Bloedel JR.** Grasping component alterations and limb transport. *Exp Brain Res* 108: 486–492, 1996.
- Uno Y, Kawato M, and Suzuki R.** Formation and control of optimal trajectory in human multijoint arm movement. *Biol Cybern* 61: 89–101, 1989.
- Wolpert DM, Ghahramani Z, and Jordan MI.** Are arm trajectories planned in kinematic or dynamic coordinates?: an adaptation study. *Exp Brain Res* 103: 460–470, 1995.
- Zatsiorsky VM, Li Z, and Latash ML.** Coordinated force production in multi-finger tasks: finger interaction and neural network modeling. *Biol Cybern* 79: 139–150, 1998.